Analytical Methods

COMMUNICATION

View Article Online
View Journal | View Issue

Fast detection of paracetamol on a gold nanoparticle–chitosan substrate by SERS

Cite this: *Anal. Methods*, 2014, **6**, 3564

Received 13th March 2014
Accepted 25th March 2014

DOI: 10.1039/c4ay00635f

www.rsc.org/methods

Elias de Barros Santos,[a] Elaine Cristina Nogueira Lopes Lima,[b] Cristine Santos de Oliveira,[a] Fernando Aparecido Sigoli[a] and Italo Odone Mazali*[a]

A fast method for detecting pharmaceutical drugs, such as paracetamol, by surface-enhanced Raman spectroscopy (SERS) using a gold nanoparticle substrate was studied. Gold nanoparticles were synthesized using chitosan (AuNP–chitosan) as a reductant and capping agent and subsequently deposited on glass slides as a thin film. The SERS performance of AuNP–chitosan films was evaluated using methylene blue (MB, 10^{-6} mol L^{-1}) as a SERS probe molecule. The method is based on drop-drying an analyte solution (paracetamol, 10^{-3} mol L^{-1}) onto a substrate surface and subsequently analyzing by Raman spectroscopy. The spectra were obtained in 10 seconds with two accumulations and exhibit a high signal-to-noise ratio. This preliminary study supports the AuNP–chitosan substrate as a SERS sensor, for a convenient analytical method for detection of paracetamol and other pharmaceutical drug molecules.

Introduction

The occurrence and fate of pharmaceutical compounds in an aquatic environment has been recognized as one of the emerging issues in environmental chemistry.[1,2] Depending on the area many of these compounds are found in concentrations of around μg kg^{-1}, ng kg^{-1} and so on.[1,2] For example, 4-hydroxyacetanilide, also named paracetamol and acetaminophen, is one of the most frequently used analgesic and antipyretic drugs.[3] Like other analgesic drugs, paracetamol gets rapidly absorbed and distributed after oral administration and it is easily excreted in urine.[4] The presence of pharmaceuticals from human medical care in an aquatic environment may, however, also be caused by other sources such as landfill leachates,[5] disposal of unused medication *via* the toilet,[6] and manufacturing residues.[7] Several studies have shown some evidence that substances of pharmaceutical origin are often not eliminated during waste water treatment and also not biodegraded in the environment.[8,9] In this context, fast methods for determination of this kind of compounds can be an efficient strategy to investigate the quality of water after waste water treatment. For this purpose, recently, several investigations have shown some methodologies, by using SERS/Raman spectroscopy as an analytical tool, to detect molecules that are found in samples collected from aquatic environments.[10–12]

Raman spectroscopy is a fast and non-destructive technique and it can be carried out directly on the samples without any extensive sample preparation.[13,14] However, the low strength of the Raman signal is a limitation to detect molecules in low concentrations, since the Raman line is directly proportional to the concentration of the scattering component of a sample in a laser beam.[15,16] Moreover, the intensity of Raman scattering (characterized by the Raman cross-section) can vary by many orders of magnitude depending on the molecules under study and the incident laser beam. It is important to clarify here that the conditions for a molecule to be a "good Raman scattering" one is not enough to make it a good SERS probe.[15,16] Then, a study of the individual Raman spectrum of the target molecule under SERS conditions is an important step before proceeding with the application.

The challenge of detecting chemicals in low concentrations has been overcome by using surface enhanced Raman spectroscopy.[17,18] SERS relies on electronic and chemical interactions among the excitation laser, the molecule of interest, and the SERS substrate.[14] The nature of SERS enhancement of the Raman signal is caused by two contributing mechanisms.[14,15] First is the electromagnetic mechanism (long-range), which is a consequence of the interaction of the electric field (from the incident radiation) with the electrons in the metal surface, leading to the excitation of surface plasmons. The second mechanism (short-range) is due to charge-transfer from the metal to the molecules adsorbed on the metallic substrate surface. The maximum SERS enhancement, up to 10^{14}-fold the normal Raman signal, typically is observed at specific positions

[a]*Functional Materials Laboratory – Institute of Chemistry –University of Campinas – UNICAMP, P.O. Box 6154, Campinas, SP, Brazil, Zip Code 13083-970. E-mail: mazali@iqm.unicamp.br; Fax: +55 19 35213023; Tel: +55 19 35213164*

[b]*Laboratory of Synthesis and Characterization of Materials, Department of Chemistry/CCET – Federal University of Sergipe – UFS, São Cristóvão – SE, Brazil, 49100-000*

in the substrate surface (hot spots) and only those molecules adsorbed there can gain from it. Substrates that sustain high magnitude of the SERS enhancement have been applied in the detection of biological and chemical species in several kinds of samples with high sensitivity.[16–18]

The stabilization of Ag and Au nanoparticles with reductant and capping agents has been reported as a promising strategy to prepare stable and efficient SERS substrates.[10,11,19–21] Chen *et al.* demonstrated a simple method to detect sulfide in environmental and biological media at the nM level by SERS using a silver nanoparticle substrate.[10] Péron *et al.* described a quantitative SERS sensor based on gold nanoparticles for the environmental analysis of naphthalene in the range of 1–20 ppm.[11] In the present communication, a simple and fast SERS sensing method for the detection of pharmaceutical drugs, such as paracetamol, with high sensitivity is reported. For this purpose, gold nanoparticles were synthesized using chitosan as a reductant and capping agent, and subsequently deposited as a thin film on glass slides. The SERS properties of the material were probed using methylene blue as a Raman probe molecule. Thus, to evaluate the possibility of employing the AuNP–chitosan substrate in future applications, as a platform in the detection and analysis of pharmaceutical drugs, it was tested to detect paracetamol by a simple and fast method.

Experimental

The chitosan powder sample (high molecular weight, 78% deacetylated) was acquired for free from C. E. Roeper, Hamburg – Germany. Tetrachloroauric(III) acid, 3-mercaptopropyl-trimethoxysilane (MPTMS), methylene blue and 4-hydroxyacetanilide (paracetamol) were purchased from Sigma-Aldrich. All chemicals were used without further purification. All glassware were cleaned with piranha solution (4 : 1 sulphuric acid : hydrogen peroxide) before using and then rinsed thoroughly with deionized water.

AuNPs were prepared following the procedure reported elsewhere with some modifications.[22] Briefly, a solution of chitosan 1 mg mL^{-1} was prepared by dissolving the polymer in acetic acid solution (pH = 2.5). Due to the low solubility of chitosan, the mixture was kept under stirring for 8 h to obtain a clear solution. A mixture of 6 mL solution of 10^{-3} mol L^{-1} tetrachloroauric(III) acid and 36 mL solution of 1 mg mL^{-1} chitosan was prepared. The AuNP–chitosan synthesis was carried out under stirring at 100 °C for 10 min, resulting in a red color solution.

Microscope regular glass slides were cut in pieces of 1.2 cm^2, cleaned, and their surfaces were modified following the procedure reported elsewhere, but in the present work using MPTMS.[23] The AuNP–chitosan films were prepared by dropping 100 μL of AuNP solution onto thiol group modified glass pieces. For solvent evaporation the pieces were placed in an oven at 50 °C for 15 min. To complete the film preparation this procedure was repeated two more times, drop-drying a total volume of 300 μL for each AuNP–chitosan film prepared. Before the second and third AuNP–chitosan deposition the films were washed with deionized water to displace any residual material of the synthesis and dried with N_2 flow.

UV-visible absorption spectra of the AuNP–chitosan solution and of the AuNP–chitosan films were collected on an Agilent Cary probe 50 UV-vis spectrometer. High resolution transmission electron microscopy (HRTEM) images were obtained using a JEOL JEM-3010 microscope (300 kV, 1.7 Å point resolution). The sample was prepared by drop-drying the AuNP–chitosan solution on a holey carbon coated Cu grid. SERS spectra were acquired using a confocal Jobin-Yvon T64000 Raman spectrometer system, equipped with a liquid-N_2-cooled CCD. The excitation source was a laser at 633 nm. The laser power at the sample surface was about 7.2 mW. The laser was focused with a 100× focal-lens objective to a spot of about 1 μm. For all measurements, the laser exposure time was 10 s with two accumulations. An aliquot of 50 μL of MB (10^{-6} mol L^{-1}) aqueous solution was dropped onto the 1.2 cm^2 AuNP–chitosan film surface. The film was dried in an air atmosphere. After that, the sample was ready to be analyzed. The same procedure was used to detect paracetamol (10^{-3} mol L^{-1}).

Results and discussion

Fig. 1(a) shows the UV-vis absorption spectrum of the AuNP–chitosan solution with a surface plasmon band at 525 nm. This is the standard optical signature for the formation of AuNP spheres in solution. A representative AuNP–chitosan film shows the surface plasmon band at 537 nm, indicating a red shift of 12 nm in the absorption maximum (Fig. 1(b)). This red shift is caused due to an increase in the refractive index of the media surrounding metallic nanoparticles.[24,25] The UV-vis spectral profile of the chitosan solution (Fig. 1(c)) does not show any absorption band at the UV-vis range. As observed in the HRTEM image in Fig. 2(a) the AuNPs are immersed into the chitosan structure forming a composite. Measuring the AuNP diameter, in different HRTEM images, it is obtained as an average size distribution of 5.2 nm (Fig. 2(b)). The narrow size distribution

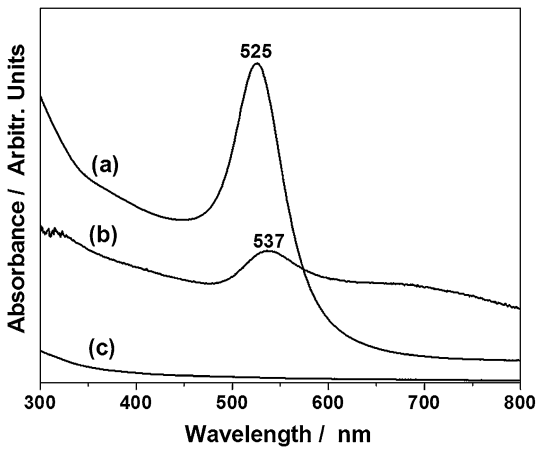

Fig. 1 UV-visible absorption spectra of (a) AuNP–chitosan solution, (b) a representative film prepared with AuNP–chitosan, and (c) chitosan solution.

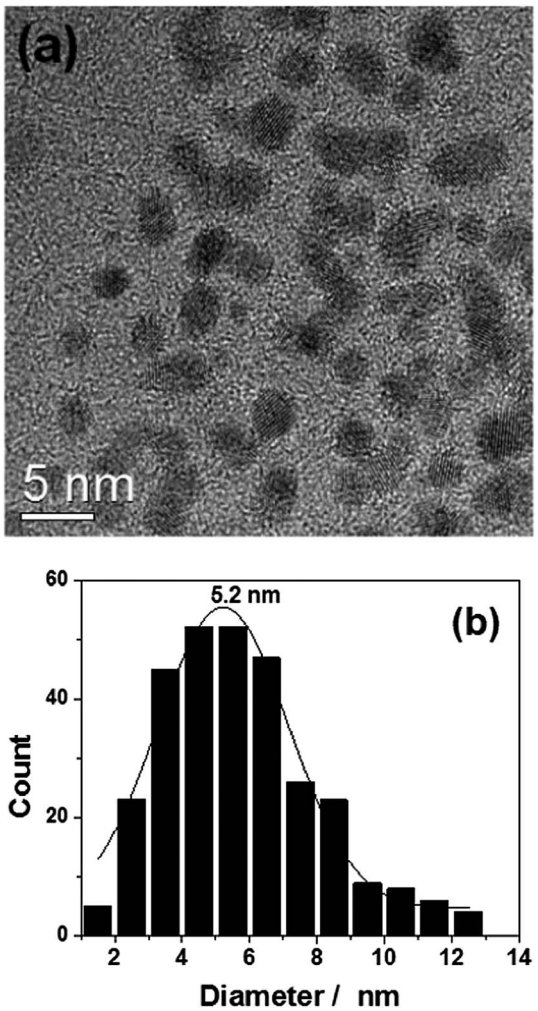

Fig. 2 (a) HRTEM image showing the AuNPs in the chitosan structure and (b) histogram of the AuNP average size distribution in the chitosan structure.

(1.5–12.5 nm) indicates that chitosan plays an important role in controlling the AuNP size as well as provides a high density of gold nanoparticles on its structure. This condition is related to the short distance among the AuNPs immersed into the chitosan structure, being an appropriate condition to plasmon coupling, which promoted Raman signal enhancement.

As shown in the literature, stable gold nanoparticles can be easily synthesized with excellent size control using chitosan as a reductant and capping agent.[26,27] Its dual role is a great advantage, once it is not necessary add other compounds to promote the reaction. Despite the widespread use of chitosan in the gold nanoparticles synthesis, the reaction mechanism has not been explained. In the present work, the synthesis of gold nanoparticles using chitosan was conducted in acetic acid solution. Under this condition, chitosan is soluble and the amine groups can be protonated ($-NH_3^+$); consequently, this biopolymer gets a positive residual charge. Then, these groups can attract the $AuCl_4^-$ ions from the solution, suggesting that they are the sites where the reduction step takes place to size-controllable AuNPs. Finally, the chitosan chains, loaded with AuNPs, self-assemble into larger structures as shown in Fig. 2(a). The overall reaction could be represented as illustrated in Fig. 3 according to our results and to some related studies.[26,27]

To evaluate the SERS efficacy of the AuNP–chitosan film, Raman measurements were conducted employing MB as the model molecule. As shown in Fig 4(a), it is clear that the characteristic Raman bands of MB are very weak to be observed and the spectrum was multiplied twenty times. The bands of MB at 1622 and 446 cm^{-1}, which have been assigned to C–C stretching and C–N–C skeletal bending, respectively, are the most intense bands in the SERS spectrum (Fig. 4(b)). This result indicates that the MB molecules were adsorbed on the AuNP–chitosan substrate.[28,29] The bands at 236 and 306 cm^{-1} that were not observed in the powder MB spectrum can be ascribed to Au–N and Au–S stretching of the Au–MB complex, respectively.[29,30] The bands at 360, 670, 1031, and 1230 cm^{-1} are observed only in the MB SERS spectrum (Fig. 4(b)). At the same time, the intensities of the bands at 478 and 888 cm^{-1} are very prominent under the SERS conditions, which is strong evidence of this enhancement effect.

To check the repeatability of the SERS spectra, measurements were made in five different points, randomly chosen, in the same AuNP–chitosan film. The MB Raman signature is observed in all collected SERS spectra (Fig. 5). The difference was only between the relative intensities of the spectra collected from point-to-point, while the spectral position and the full width of Raman bands show no noticeable difference (Fig. 5). The band at 1622 cm^{-1} exhibits the highest intensity, indicating that this band can be used as an MB reference in future analyses.

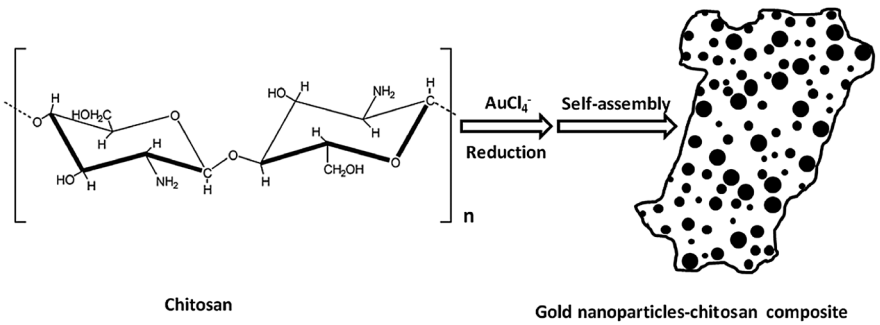

Fig. 3 Simplified schematic representation of the formation of the AuNP–chitosan composite.

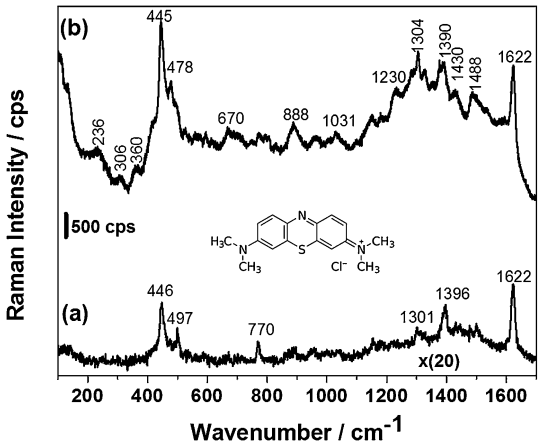

Fig. 4 (a) Raman spectrum of solid methylene blue powder and (b) SERS spectrum of 10^{-6} mol L^{-1} methylene blue dropped onto a AuNP–chitosan film.

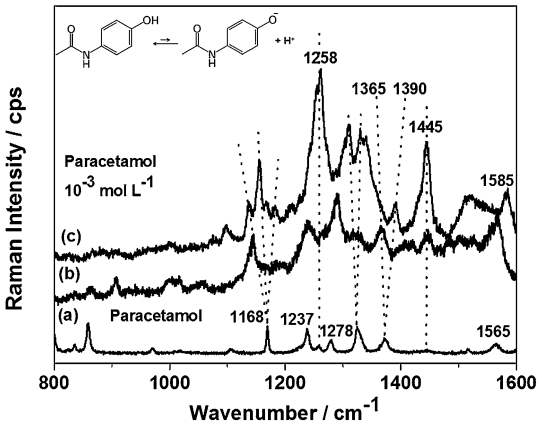

Fig. 6 (a) Raman spectrum of paracetamol powder, (b) and (c) SERS spectra of 10^{-3} mol L^{-1} paracetamol recorded onto a AuNP–chitosan film. The inset shows the deprotonation equilibrium of paracetamol and its conjugated base in water.

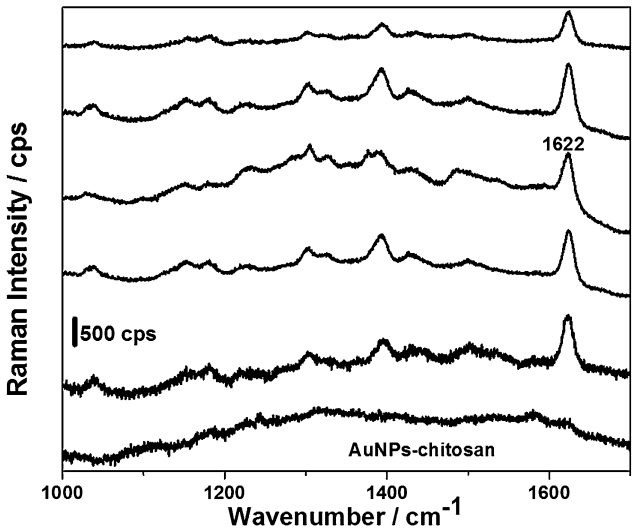

Fig. 5 SERS spectrum of the AuNP–chitosan substrate and SERS spectra of 10^{-6} mol L^{-1} methylene blue onto a AuNP–chitosan film recorded in five different points.

The Raman signal scattered from chitosan is very weak and it does not interfere with the SERS spectra of the MB model molecule (Fig. 5). This is an interesting result, indicating that this kind of substrate can be employed to detect molecules without any interference from the substrate background. As a demonstration of a practical application of the above AuNP–chitosan substrate, it was tested as a SERS sensor to detect paracetamol. Fig. 6 shows the measured SERS spectra for paracetamol powder and for paracetamol after drop-drying 50 μL of 10^{-3} mol L^{-1} solution on the AuNP–chitosan substrate. The SERS spectra differ mainly in intensity and positions when comparing with the Raman spectrum of the paracetamol powder. Also, the SERS spectra differ from each other (Fig. 6(b) and (c)). This can be explained based on paracetamol's chemical structure,[31] which can undergo deprotonation and achieve a stable equilibrium in water (inset of Fig. 6). Both structures, paracetamol and its conjugated base (oxyanion), can interact with the AuNP–chitosan substrate in different ways due to their different charges. In that situation molecules can be differently orientated on the sensor surface, resulting in different intensities and positions of some Raman bands as observed in Fig. 6.

The band at 1168 cm^{-1} for σ^{ip}(HCC, ip: in-plane) and for ν(CC) is shifted to 1145 and 1154 cm^{-1} and also is observed in the SERS spectrum in Fig. 6(c), indicating that there are molecules attached on the AuNP–chitosan substrate surface with different orientations.[32,33] The band at 1237 cm^{-1} for ν(CC) and σ^{ip}(HOC) is observed in both SERS spectra, appearing as the shoulder in the spectrum in Fig. 6(c). The band at 1258 cm^{-1} for ν(C–O), σ^{ip}(HCC) and ν(CC) appears only in the spectrum in Fig. 6(c) as the highest one, indicating that the SERS effect is operating on the system. The band at 1325 cm^{-1}, attributed to the amide III band (C–N stretch/C–N–phenyl stretch/C–N–H band), is split and becomes more intense in Fig. 6(c). The band at 1371 cm^{-1} for $\sigma^{s}(CH_3$, s: symmetric) appears in different positions in the SERS spectra; unlike this band, the band at 1445 cm^{-1} for $\sigma^{as}(CH_3$, as: asymmetric) is observed in the same position in the SERS spectra, but it is much more intense in Fig. 6(c). The band at 1565 cm^{-1} for σ^{ip}(HNC) and ν(CC) is observed only in Fig. 6(b), while the band at 1585 cm^{-1} for ν(CC) and σ^{ip}(HNC) is observed only in Fig. 6(c).[33] The band at 907 cm^{-1} observed only in Fig. 6(b) could not be assigned, since any band was observed in this position in the paracetamol powder Raman spectrum. These changes observed in the SERS spectra bands are correlated with orientation differences in the paracetamol molecules adsorbed on the AuNP–chitosan SERS sensor. The high intensity observed for some bands, under the SERS conditions, indicates that the substrate is a promising sensitive sensor to detect paracetamol even in concentrations below 10^{-3} mol L^{-1}. This kind of a SERS sensor has potential applications in the analytical field and the straightforward procedure used has several advantages as a fast and efficient method.

Conclusions

AuNPs were synthesized by a simple and convenient method using chitosan as a reductant and capping agent. The AuNP–chitosan composite is easily deposited on a glass slide forming a film, which exhibited excellent performance as a SERS substrate. The AuNP–chitosan film showed sensitivity to detect MB in low concentrations by SERS. It was employed as a SERS sensor to detect and identify paracetamol by drop-drying 50 μL onto the substrate surface. This methodology is simple, fast and cost-effective. Also, the originality and advantage of this SERS-active substrate reside in the fact that the chitosan Raman signal does not interfere with the Raman spectra of the analytes. In the near future, AuNP–chitosan can be employed as a sensor of other pharmaceutical drugs by using the same methodology, even in low concentrations.

Acknowledgements

EBS thanks FAPESP for a post-doc fellowship. The authors would like to thank the FAPESP, CAPES and CNPq for financial support. Contributions from the Multiuser Laboratory of Advanced Optical Spectroscopy (LMEOA/IQ/UNICAMP) for Raman facilities and the Brazilian Nanotechnology National Laboratory (LNNano, Campinas-SP, Brazil) for HRTEM facilities are also gratefully acknowledged. This is a contribution of the National Institute of Science and Technology in Complex Functional Materials (CNPq-MCT/FAPESP).

References

1 B. Halling-Sorensen, N. Nielsen, P. F. Lansky, F. Ingersley, L. Hansen, H. C. Lutzhoft and S. E. Jorgensen, *Chemosphere*, 1998, **36**, 357.
2 C. G. Daughton and T. A. Ternes, *Environ. Health Perspect.*, 1999, **107**, 907.
3 K. Klimova and J. Leitner, *Thermochim. Acta*, 2012, **550**, 59.
4 J. Parojcic, K. Karljikovic-Rajic, Z. Duric, M. Jovanovic and S. Ibric, *Biopharm. Drug Dispos.*, 2003, **24**, 309.
5 J. V. Holm, K. Rugge, P. L. Bjerg and T. H. Christensen, *Environ. Sci. Technol.*, 1995, **29**, 1415.
6 T. A. Ternes, *Water Res.*, 1998, **32**, 3245.
7 K. Reddersen, T. Heberer and U. Dunnbier, *Chemosphere*, 2002, **49**, 539.
8 C. Zwiener, T. Glauner and F. H. Frimmel, *High Resolut. Chromatogr.*, 2000, **23**, 474.
9 H. R. Buser, T. Poiger and M. D. Muller, *Environ. Sci. Technol.*, 1999, **33**, 2529.
10 L.-X. Chen, D.-W. Li, L.-L. Qu, Y.-T. Li and Y.-T. Long, *Anal. Methods*, 2013, **5**, 6579.
11 O. Péron, E. Rinnert, T. Toury, M. L. Chapelle and C. Compere, *Analyst*, 2011, **136**, 1018.
12 R. A. Alvarez-Puebla and L. M. Liz-Marzan, *Angew. Chem., Int. Ed.*, 2012, **51**, 11214.
13 M. Fleischmann, P. J. Hendra and A. J. McQuillan, *Chem. Phys. Lett.*, 1974, **26**, 63.
14 E. C. Le Ru and P. G. Etchegoin, *Principles of Surface-enhanced Raman Spectroscopy*, Elsevier, Amsterdam, 2009.
15 R. Aroca, *Surface-enhanced Vibrational Spectroscopy*, John Wiley & Sons, Southern Gate, 2006.
16 Y. Zhang, S. Liu, L. Wang, X. Qin, J. Tian, W. Lu, G. Chang and X. Sun, *RSC Adv.*, 2012, **2**, 538.
17 G. Moula and R. F. Aroca, *Anal. Chem.*, 2011, **83**, 284.
18 W. W. Yu and I. M. White, *Analyst*, 2012, **137**, 1168.
19 W. L. Zhai, D. W. Li, L. L. Qu, J. S. Fossey and Y. T. Long, *Nanoscale*, 2012, **4**, 37.
20 M. Alsawafta, S. Badilescu, M. Packirisamy and V. V. Truong, *React. Kinet., Mech. Catal.*, 2011, **104**, 437.
21 K. Esumi, N. Takei and T. Yoshimura, *Colloids Surf., B*, 2003, **32**, 117.
22 M. Potara, D. Maniu and S. Astilean, *Nanotechnology*, 2009, **20**, 315602.
23 E. B. Santos, F. A. Sigoli and I. O. Mazali, *Vib. Spectrosc.*, 2013, **68**, 246.
24 Y. Q. Wang, W. S. Liang and C. Y. Geng, *Nanoscale Res. Lett.*, 2009, **4**, 684.
25 E. F. S. Vieira, A. R. Cestari, E. B. Santos and F. S. Dias, *J. Colloid Interface Sci.*, 2005, **289**, 42.
26 Y.-C. Cheng, C.-C. Yu, T.-Y. Lo and Y.-C. Liu, *Mater. Res. Bull.*, 2012, **47**, 1107.
27 T. T. Nhung, Y. Bu and S.-W. Lee, *J. Cryst. Growth*, 2013, **373**, 132.
28 G. N. Xiao and S. Q. Man, *Chem. Phys. Lett.*, 2007, **447**, 305.
29 C. M. Ruan, W. Wang and B. H. Gu, *J. Raman Spectrosc.*, 2007, **38**, 568.
30 Y. Peng, Z. Niu, W. Huang, S. Chen and Z. Li, *J. Phys. Chem. B*, 2005, **109**, 10880.
31 M. A. Elbagerma, G. Azimi, H. G. M. Edwards, A. I. Alajtal and I. J. Scowen, *Spectrochim. Acta, Part A*, 2010, **75**, 1403.
32 B. Chazallon, Y. Celik, C. Focsa and Y. Guinet, *Vib. Spectrosc.*, 2006, **42**, 206.
33 J. B. Nanubolu and J. C. Burley, *Mol. Pharmaceutics*, 2012, **9**, 1544.

